FEBS Letters 580 (2006) 256–260

Improved gating of a chimeric α7-5HT$_{3A}$ receptor upon mutations at the M2–M3 extracellular loop

Mar Castillo, José Mulet, José Antonio Bernal, Manuel Criado, Francisco Sala, Salvador Sala*

Instituto de Neurociencias de Alicante, Universidad Miguel Hernández-C.S.I.C., 03550-Sant Joan d'Alacant, Alicante, Spain

Received 14 October 2005; revised 1 December 2005; accepted 6 December 2005

Available online 12 December 2005

Edited by Peter Brzezinski

Abstract **Acetylcholine-evoked currents of the receptor chimera α7-5HT$_{3A}$ V201 expressed in *Xenopus* oocytes are strikingly small when compared to the amount of α-bungarotoxin binding sites detected at the oocyte membrane. Since the chimeric receptor is made of the extracellular N-terminal region of the rat α7 nicotinic acetylcholine receptor and the C-terminal region of the mouse 5-HT$_{3A}$ receptor, which includes the ion channel, we hypothesized that communication between these two regions was not optimal. Here, we show that mutating to aspartate several adjacent positions in the M2–M3 extracellular linker increases current amplitudes to different extents, thus confirming the important role of this region on receptor gating.**

Keywords: α7 Nicotinic receptor; 5-HT$_{3A}$ receptor; V201 chimera; M2–M3 linker; Aspartate; Gating

1. Introduction

Cys-loop receptors are ligand-gated ion channels that mediate fast synaptic transmission in nerve and muscle cells (reviewed in [1,2]). Agonist binding to the receptor triggers a signal that must be transmitted to the channel gate through conformational changes [3]. The α7-5HT$_{3A}$ receptor (V201 hereafter) is a chimera which has been very useful for studying the electrophysiological properties of ligand-gated receptors [4,5]. This chimera is made of two different receptors: (a) the extracellular N-terminal region of the rat α7 nicotinic acetylcholine receptor (nAChR) until Val201, including the acetylcholine (ACh) and α-bungarotoxin (α-Bgt) binding sites and (b) the C-terminal region of the mouse 5-HT$_{3A}$ receptor (5-HT$_{3A}$R), which includes the ion channel forming transmembrane segments and the large cytoplasmic loop [4]. Accordingly, ACh activates channels whose properties mimic the ones of 5-HT$_{3A}$Rs. Previous studies have shown that functional coupling requires compatibility at the interface of the binding and pore domains [6]. Strikingly, when V201 receptors were expressed in *Xenopus* oocytes we observed that ACh-evoked currents were very small when compared to the amount of α-Bgt binding sites detected at the oocyte membrane. We hypothesized that communication between the two regions of the different receptors was not optimal, perhaps because the M2–M3 linker, which is contributed by the 5-HT$_{3A}$R, was not able to adequately receive the signal from the α7 nAChR extracellular region. This incapacity could be due to the absence of a negatively charged residue at the M2–M3 linker, since we have shown previously that the negatively charged Asp266 residue in the M2–M3 linker of α7 nAChRs [7] and an equivalent residue in other neuronal nAChRs [8] are involved in coupling agonist binding and gating. Therefore, to test this hypothesis we introduced an aspartate residue at different adjacent positions of the V201 M2–M3 linker and characterized the resultant channels.

2. Materials and methods

2.1. Generation of mutants of the V201 chimera

The V201 cDNA was gently provided by Dr. K.T. Dineley and cloned in a derivative of the pSP64T vector [9] containing part of the pBluescript polylinker. To generate the mutants, we annealed single-stranded oligonucleotides with the desired sequences and proper single strand ends which could be easily ligated to the ends generated by restriction enzymes present in the original cDNA sequence such as *Nae*I (corresponding to amino acids P261 and A262), *Kpn*I (amino acids G265 and T266) and *Acc*I (amino acids V271 and Y272). Wild-type rat α7 was also used in some occasions for the sake of comparison.

2.2. Oocyte expression

Capped mRNA was synthesized in vitro using SP6 RNA polymerase, the mMESSAGE mMACHINE kit (Ambion) and the pSP64T derivative mentioned above. Defoliculated *Xenopus leavis* oocytes were injected with 5 ng of total cRNA in 50 nl of sterile water. All experiments were performed within 3–4 days after cRNA injection.

2.3. [^{125}I]α-bungarotoxin *binding assays*

Specific surface expression of [^{125}I]α-Bgt binding sites was tested with 10 nM [^{125}I]α-Bgt as described [9]. Briefly, oocytes located in 24-well plates were incubated in Barth's buffer with 10 nM [^{125}I]α-Bgt for 2 h at 18 °C in a final volume of 300 μl. At the end of the incubation, unbound [^{125}I]α-Bgt was removed, oocytes were passed to 6-well plates, washed five times with 4 ml Barth buffer and bound radioactivity was counted. Non-specific binding was determined using non-inoculated oocytes.

2.4. Electrophysiological recordings

Electrophysiological recordings were done as described previously [10]. Functional expression of each construct was estimated as the peak ionic current evoked by 1 s application of 1 mM ACh at −80 mV, and no correction per desensitization was made. All experiments were done at room temperature (22 °C).

*Corresponding author. Fax: +34 965919561/47.
E-mail address: salvador.sala@umh.es (S. Sala).

Abbreviations: ACh, acetylcholine; nAChR, nicotinic acetylcholine receptor; α-Bgt, α-bungarotoxin; 5-HT$_{3A}$R, serotonergic receptor, subtype 3A

0014-5793/$32.00
doi:10.1016/j.febslet.2005.12.010

2.5. Data analysis

Dose–response curves were fitted using a nonlinear least squares algorithm to the Hill equation: $I/I_{max} = 1/[1 + (EC_{50}/C)^{nH}]$, where EC_{50} is the agonist concentration that elicits the half-maximal response, nH is the Hill coefficient and C is the agonist concentration. The curves were also fitted to the steady-state solution of a four state linear model: $R \leftrightarrow RL \leftrightarrow RL_2 \leftrightarrow OL_2$ where the first two transitions are assumed to be identical binding steps with a binding constant $B = k_1/k_{-1}$ and the last one is a gating transition with a gating constant $G = \beta/\alpha$, i.e.

$$I/I_{max} = 1/[1 + 1/G + 2/(G \cdot B \cdot C) + 1/(G \cdot (B \cdot C)^2)]$$

Statistical significance of the difference between two means was evaluated by computing the P-level of the two-sided t-test with the program Prism, GraphPad Software, Inc.

3. Results and discussion

3.1. Involvement of M2–M3 loop in the functional efficiency of V201 receptors

ACh-evoked currents of rat α7 and V201 receptors expressed in *Xenopus* oocytes were similar in peak amplitude (Fig. 1A). By contrast, the amount of α-Bgt binding sites detected at the oocyte membrane was more than 60-fold larger when V201 receptors were expressed. Previous studies have shown that the dissociation constant of α-Bgt for rat α7 receptors was 0.4 nM [11] whereas for chick V201 receptors was close to 1 nM [12], and so we used 10 nM that would be enough to label more than 90% of the V201 binding sites. Surprisingly however, our determination of K_d for the rat V201 receptor was 8.8 ± 1.8 nM, thus the real number of binding sites for V201 receptors is probably even greater by a factor of two. As a consequence, the function of the V201 receptors as measured by the current to α-Bgt binding ratio was considered far from being optimal (Table 1 and Fig. 1B).

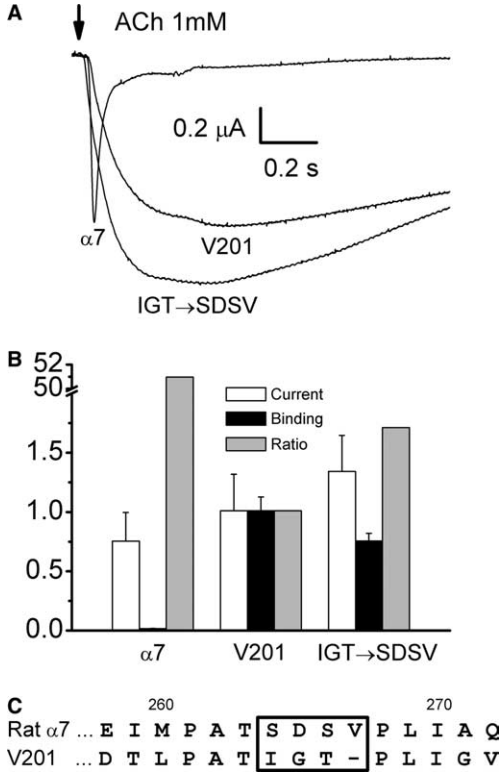

Fig. 1. Decreased function in α7-5HT$_{3A}$ V201 receptors and effect of exchanging residues in the M2–M3 linker. (A) Currents obtained by applying a pulse of 1 mM ACh at the time indicated by the arrow. The duration of the pulse was 0.4, 1.5 and 2 s for α7, V201, and V201 with the change of IGT for SDSV (IGT → SDSV), respectively. (B) Normalized values of peak currents (white bars), [^{125}I]α-Bgt binding (black bars), and the ratio between current and α-Bgt binding for each receptor (grey bars). All data have been normalized to the mean values corresponding to V201. (C) Sequence of the M2–M3 linker in rat α7 subunits and V201. Numbering corresponds to α7. The box shows the residues in the middle of the M2–M3 linker that are different in each subunit.

Although a direct comparison between α7 and V201 channels might not be rigorous, as their channel-forming sections are made of different receptors and their activation and desensitization kinetics are very different, we considered the possibility that one of the reasons for the low current levels observed in V201 receptors could be an inadequate signal transmission between the extracellular domain of the α7 nAChR and the channel and related domains of the 5H-T$_{3A}$ receptor.

We [7,8] and others [13–16] have shown that certain residues at the M2–M3 loop are important for linking receptor binding and gating and, therefore a comparison of these regions was made in α7 and V201 receptors (Fig. 1C). Interestingly, whereas the sequences P^{261}A^{262}T^{263} and P^{268}L^{269}I^{270} (numbering according to the α7 subunit) were common for both receptors, the sequence in between was totally different, i.e, SDSV in rat α7 vs. IGT in V201. Moreover, this sequence contains the aspartate residue D^{265} previously characterized by us [7]. For this reason, we substituted the IGT sequence of the V201 receptor by the SDSV sequence corresponding to the α7 subunit. The resultant receptors showed increased current amplitudes (Fig. 1A) and slightly lower surface expression (Fig. 1B), so that the ratio of current amplitude in μA to α-Bgt binding sites in fmol/oocyte increased almost twofold in the IGT → SDSV mutant compared to V201. There was also an increase in the activation rate of the mutated chimeric receptor although it was still much slower than α7 (Fig. 1A and Table 1).

3.2. Mutations to aspartate improve the function of V201 receptors

We further explored the involvement of these residues in receptor function by mutating each one in turn to aspartate. The effect of mutation I264D was to increase the magnitude of the current without affecting expression levels (Fig. 2A), thus the current to α-Bgt binding ratio increased compared to V201. The current increased even further when the mutation to aspartate was made on the glycine residue, mutant G265D, again without much change in α-Bgt binding, thus increasing the current to α-Bgt binding ratio fourfold compared with the V201 receptor. When the threonine residue was mutated to aspartate, mutant T266D, expression levels were reduced by a factor of thirty whereas the current was only reduced by a factor of two (the K_d for α-Bgt of these mutant receptors was 1.0 ± 0.6 nM, data not shown), as a consequence, the function of those mutants was even better than the previous ones. By contrast, the double mutant G265D/T266D (that we refer simply as GT → DD), did not increase the function further. In fact it had the opposite effect, because the decrease

Table 1
Current amplitude, level of expression, efficiency and activation kinetics of the receptors

Receptor	Peak current (μA) ACh 1 mM	[^{125}I]α-Bgt binding (fmol/oocyte)	Ratio: Current/α-Bgt binding μA/(fmol/oocyte)	Rise time 10–90% (ms)
α7	0.77 ± 0.18	0.49 ± 0.05	1.68 ± 0.39 (79, 9)[a]	49 ± 9 (31)[b]
V201	1.03 ± 0.22**	33.5 ± 2.7***	0.033 ± 0.008 (47, 7)**	293 ± 28 (29)***
IGT → SDSV	1.37 ± 0.09*	24.4 ± 0.4	0.056 ± 0.005 (15, 2)	204 ± 46 (15)***
I264D	3.4 ± 0.9***	43 ± 10	0.09 ± 0.03 (28, 4)*	522 ± 44 (28)***
G265D	3.3 ± 0.3***	23.8 ± 1.5	0.14 ± 0.02 (14, 2)***	552 ± 60 (14)***
T266D	0.43 ± 0.15***	1.09 ± 0.04***	0.39 ± 0.13 (16, 2)***	410 ± 92 (14)***
GT → DD	0.049 ± 0.002***	2.1 ± 0.9***	0.025 ± 0.01 (15, 2)	N.D.

Statistical differences: $^{*}P < 0.05$, $^{**}P < 0.01$, $^{***}P < 0.001$.
V201 compared with α7, all the others compared with V201.
[a]Numbers in parentheses in this column indicate (number of oocytes, number of different donors).
[b]Number in parentheses in this column indicate (number of oocytes).

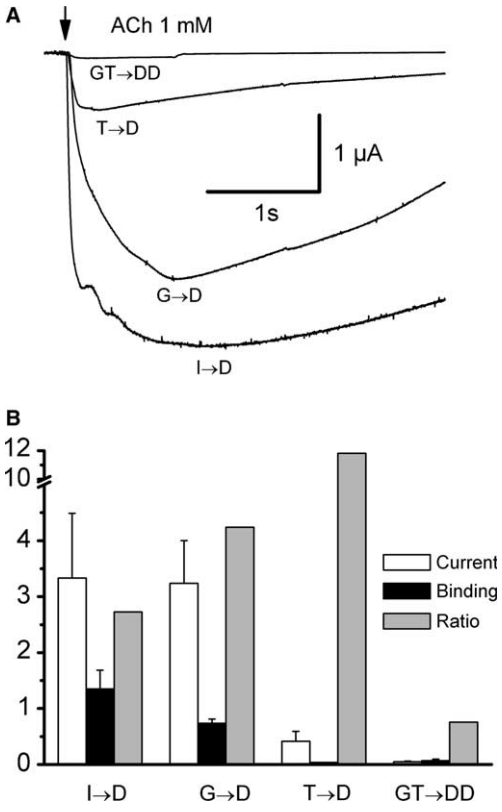

Fig. 2. Increase of function by single mutations to aspartate. (A) Currents obtained by applying a 1.5 s pulse of 1 mM ACh for different mutant receptors as indicated by the letters below the corresponding record. (B) Normalized values of peak currents (white bars), [^{125}I]α-Bgt binding (black bars), and the ratio between current and α-Bgt binding for each receptor (grey bars). All data have been normalized to the mean values corresponding to V201.

in the peak current by a factor of 21 was larger than the reduction of α-Bgt binding, by a factor of 16. Thus the function of this double mutant was even worse than that of V201 and we can conclude that the effect observed in the single mutants is not additive. Due to the small values of the peak currents, we could not determine the activation kinetics of the GT → DD receptors.

Interestingly, the increase in function of the three single mutants was not accompanied by an increase in the activation kinetics as the activation time was even larger than that for V201. Moreover, neither the selectivity nor the voltage dependence of the open mutated receptors were changed, as determined by the reversal potential and rectification ratio obtained in experiments with ramp voltages (Fig. 3).

3.3. Mutations to aspartate decrease acetylcholine EC_{50} and increase nH

To determine whether the mutations had affected the sensitivity to ACh, we obtained concentration response curves (Fig. 4). In these experiments, we compared V201 with the two single mutants that showed the largest improvement in function, i.e., G265D and T266D. For all three receptors, 1 mM ACh was almost an equivalent concentration because it was very close to the saturating value. The mutated receptors

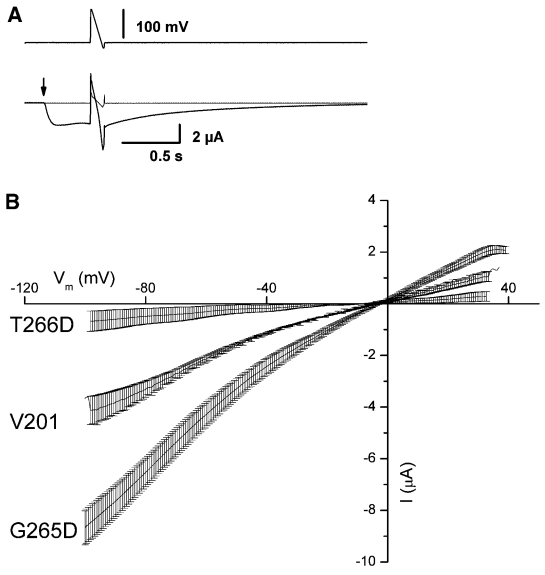

Fig. 3. Current–voltage curves for V201 and aspartate mutants. (A) Voltage and current traces obtained in a typical experiment. The upper record is the membrane potential, held at −80 mV, then stepped to +40 mV and maintained for 10 ms, and then ramped down from +40 to −100 mV in 100 ms, finally, after 10 ms more it is stepped back to the holding potential of −80 mV. The lower records are current traces, the first one is the leak record obtained without applying ACh, and the second one is obtained when ACh 1 mM is applied at the time indicated by the arrow. (B) Open current–voltage relationships for V201 and the mutants G265D and T266D. For each receptor the lines are averages from four different oocytes and the error bars are the standard errors.

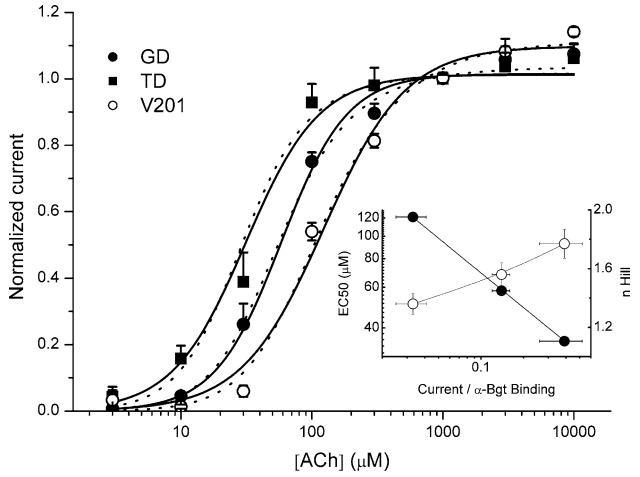

Fig. 4. ACh concentration–current curves. Peak currents were normalized to the value of 1 mM ACh. Solid lines are fits to the Hill equation with the following (I_{max}, EC_{50}, nH) values: (1.06 ± 0.01, 109 ± 6 μM, 1.4 ± 0.1) for V201 (open circles); (1.03 ± 0.01, 57 ± 2 μM, 1.6 ± 0.1) for G265D (solid circles); and (1.02 ± 0.01, 31 ± 1 μM, 1.8 ± 0.1) for T266D (solid squares). Dotted lines are fits to the steady-state solution of the four states kinetic model with an arbitrary scale factor and a fixed value of the binding constant equal for all receptors. The inset shows the dependence of the resulting EC_{50} (solid dots) and Hill coefficients (open dots), on the current to α-Bgt binding ratio, for the three receptors. The scale for the Hill coefficient is linear, and the other two are logarithmic. The solid line across the EC_{50} values is the fit of the data to an inverse square root function. The line across the nH values is just a spline line.

had concentration–response curves shifted to the left compared with V201, having the one with the most improved function (T266D) the smaller EC_{50} value. In fact, this correlation of EC_{50} with function can be well fitted by an inverse square root function as shown in the inset in Fig. 4. This result is what predicts the four state model as a consequence of an increase in receptor efficacy, i.e. an increase in the gating constant (β/α). We also observed an increase in the Hill coefficient in the mutations with improved function. This dependence of the Hill coefficient on the current/α-Bgt binding ratio is also shown in the inset. Again, the increase in nH is also predicted by the model, simply as a consequence of an increase in the gating constant [17].

An additional test confirms that function improvement results from an increase in receptor gating without changing the ability to bind the ligand. In Fig. 4, we show that the dose–response data can be fitted by the steady-state solution of the simple four state kinetic model described in Section 2 (dotted lines), even with the restriction of keeping the binding constant fixed and equal for all three receptors.

Single channel conductances as low as 0.76 pS have been reported for $5HT_{3A}$ receptors [18], whereas values as high as 48 pS have been reported for rat α7 receptors [19], thus suggesting that this could be a major determinant of the low efficiency of the V201 receptors. In fact, replacement of three arginine residues unique to the large cytoplasmic region of the $5\text{-}HT_{3A}$ subunit by their $5\text{-}HT_{3B}$ subunit counterparts strongly increases single-channel conductance [18]. In addition to this factor, our results suggest that the gating mechanism may be flawed in V201 receptors, due to the lack of an aspartate residue in the M2–M3 linker that is conserved in α7 subunits of nAChRs. This emphasizes the importance of the connection between the extracellular domains of the α7 subunit, probably loops 2 and 7, see [20], and the M2–M3 linker, and its independence of the surrounding domains that make up the $5\text{-}HT_{3A}$ channel. Moreover, improvement of channel function is observed with the residue located at three different positions of the mentioned region, suggesting that the coupling admits a certain degree of flexibility with respect to the location of the negative charge. On the other hand, the quantitative differences observed between the mutants suggest that location of the aspartate residue at one of them (T^{266}) has the optimal coupling.

Acknowledgments: This work was supported by Research Grants from the Ministry of Education of Spain (BMC2002-00972 and SAF2002-00209), and the Generalitat Valenciana (CTIDIB/2002/138 and GRUPOS03/038). The excellent technical assistance of Susana Gerber is appreciated. We thank Dr. K. Dineley for kindly providing the V201 cDNA.

References

[1] Lindstrom, J.M. (2003) Nicotinic acetylcholine receptors of muscles and nerves: comparison of their structures, functional roles, and vulnerability to pathology. Ann. N.Y. Acad. Sci. 998, 41–52.
[2] Lester, H.A., Dibas, M.I., Dahan, D.S., Leite, J.F. and Dougherty, D.A. (2004) Cys-loop receptors: new twists and turns. Trends Neurosci. 27, 329–336.
[3] Doyle, D.A. (2004) Structural changes during ion channel gating. Trends Neurosci. 27, 298–302.
[4] Eisele, J.L., Bertrand, S., Galzi, J.L., Devillers-Thiery, A., Changeux, J.P. and Bertrand, D. (1993) Chimaeric nicotinic-serotonergic receptor combines distinct ligand binding and channel specificities. Nature 366, 479–483.
[5] Corringer, P.J., Bertrand, S., Bohler, S., Edelstein, S.J., Changeux, J.P. and Bertrand, D. (1998) Critical elements determining diversity in agonist binding and desensitization of neuronal nicotinic acetylcholine receptors. J. Neurosci. 18, 648–657.
[6] Bouzat, C., Gumilar, F., Spitzmaul, G., Wang, H.L., Rayes, D., Hansen, S.B., Taylor, P. and Sine, S.M. (2004) Coupling of agonist binding to channel gating in an ACh-binding protein linked to an ion channel. Nature 430, 896–900.
[7] Campos-Caro, A., Sala, S., Ballesta, J.J., Vicente-Agullo, F., Criado, M. and Sala, F. (1996) A single residue in the M2–M3 loop is a major determinant of coupling between binding and gating in neuronal nicotinic receptors. Proc. Natl. Acad. Sci. USA 93, 6118–6123.
[8] Rovira, J.C., Vicente-Agullo, F., Campos-Caro, A., Criado, M., Sala, F., Sala, S. and Ballesta, J.J. (1999) Gating of alpha3beta4 neuronal nicotinic receptor can be controlled by the loop M2–M3 of both alpha3 and beta4 subunits. Pflugers Arch. 439, 86–92.
[9] Krieg, P.A. and Melton, D.A. (1984) Functional messenger RNAs are produced by SP6 in vitro transcription of cloned cDNAs. Nucleic Acids Res. 12, 7057–7070.
[10] Garcia-Guzman, M., Sala, F., Sala, S., Campos-Caro, A. and Criado, M. (1994) Role of two acetylcholine receptor subunit domains in homomer formation and intersubunit recognition, as revealed by alpha 3 and alpha 7 subunit chimeras. Biochemistry 33, 15198–15203.
[11] Quik, M., Choremis, J., Komourian, J., Lukas, R.J. and Puchacz, E. (1996) Similarity between rat brain nicotinic alpha-bungarotoxin receptors and stably expressed alpha-bungarotoxin binding sites. J. Neurochem. 67, 145–154.
[12] Corringer, P.J., Galzi, J.L., Eisele, J.L., Bertrand, S., Changeux, J.P. and Bertrand, D. (1995) Identification of a new component of the agonist binding site of the nicotinic alpha 7 homooligomeric receptor. J. Biol. Chem. 270, 11749–11752.
[13] Rajendra, S., Lynch, J.W., Pierce, K.D., French, C.R., Barry, P.H. and Schofield, P.R. (1995) Mutation of an arginine residue in the human glycine receptor transforms beta-alanine and taurine from agonists into competitive antagonists. Neuron 14, 169–175.

[14] Lynch, J.W., Rajendra, S., Barry, P.H. and Schofield, P.R. (1995) Mutations affecting the glycine receptor agonist transduction mechanism convert the competitive antagonist, picrotoxin, into an allosteric potentiator. J. Biol. Chem. 270, 13799–13806.
[15] Bera, A.K., Chatav, M. and Akabas, M.H. (2002) GABA(A) receptor M2-M3 loop secondary structure and changes in accessibility during channel gating. J. Biol. Chem. 277, 43002–43010.
[16] Grosman, C., Salamone, F.N., Sine, S.M. and Auerbach, A. (2000) The extracellular linker of muscle acetylcholine receptor channels is a gating control element. J. Gen. Physiol. 116, 327–340.
[17] Colquhoun, D. (1998) Binding, gating, affinity and efficacy: the interpretation of structure–activity relationships for agonists and of the effects of mutating receptors. Br. J. Pharmacol. 125, 924–947.
[18] Kelley, S.P., Dunlop, J.I., Kirkness, E.F., Lambert, J.J. and Peters, J.A. (2003) A cytoplasmic region determines single-channel conductance in 5-HT3 receptors. Nature 424, 321–324.
[19] Mathie, A., Cull-Candy, S.G. and Colquhoun, D. (1991) Conductance and kinetic properties of single nicotinic acetylcholine receptor channels in rat sympathetic neurones. J. Physiol. 439, 717–750.
[20] Sala, F., Mulet, J., Sala, S., Gerber, S. and Criado, M. (2005) Charged amino acids of the N-terminal domain are involved in coupling binding and gating in {alpha}7 nicotinic receptors. J. Biol. Chem. 280, 6642–6647.